Experimental Study and Modelling of a Two-Stage Compression R744 Refrigeration System with Vapour Injection and Inter-Cooling

Javier VEGA[1*], Samuel GENDEBIEN[1], Vincent LEMORT[1]

[1] University of Liège , Energy Systems Research Unit
Liège, Belgium
* Corresponding Author
Contact Information (+3243664811, jivega@uliege.be)

ABSTRACT

Current trends in CO_2 supermarket refrigeration have leaned towards systems including parallel compression and ejectors. However, the possibilities that two-stage compression system architectures can offer remain out of the main spotlight. In this work, a condensing unit for CO_2 supermarket refrigeration is tested in a climatic chamber. The system includes a two-stage rolling piston compressor with vapor injection and inter-cooling. The condensing unit is tested in several operating conditions to characterize the system COP and overall behaviour of the system, with a special focus on the compressor performance assessment. The COP of the machine ranges from 3.6 to 1.3 for several testing conditions with an outlet gas cooler temperature varying from 24 to 40 [°*C*], at an evaporating temperature of -10 [°*C*]. The experimental results allow for calibrating a two-stage rolling piston compressor semi-empirical model. The parameters of this model are calibrated for the first time not only to predict the main mass flow rate and power consumption, but also discharge temperature and vapour injection mass flow rate. Results show that the semi-empirical model can predict three key compressor variables satisfactorily: first stage suction mass flow rate, compressor electric consumption and total discharge mass flow. The model calculates these variables with an average absolute relative deviation of 6.2% , 10.2% and 4.4%. Discharge temperature absolute error averages 8.0 [K]. However, high errors are obtained for the prediction of the injection mass flow rate. This may be explained by possible ill-defined thermodynamic states at the injection point that serve as model input. Lastly, the parameters identification procedure allows estimating the unknown second stage compression displacement volume by means of error minimization.

1. INTRODUCTION

Seven years after the 2015 F-gas regulation, the HVAC&R researchers and industry are still submitted to the challenge of finding cleaner and more efficient technologies. In the refrigeration sector, it has revived the interest in applying propane (R290), ammonia (R717) and carbon dioxide (R744), which this paper focuses on, as the refrigerant working fluid. Specifically in the food retail sector, CO_2 has been successfully established in countries that have politically enforced technological transition towards cleaner solutions. For example, it has been reported that, as in 2019, in Europe, CO_2-based supermarkets account for 14%, and that at least 3530 plants are operating in Japan (Skačanová and Battesti, 2019).

Nonetheless, a particularity of the CO_2 is that it works in high-pressure transcritical conditions when ambient temperature is high, leading to important performance losses when applied to more traditional refrigeration architectures. What has allowed this working refrigerant to be competitive and commonly adopted is the very active research surrounding it to improve its performance in warm climates. Many first attempts to efficiently apply R744 in supermarket application have converged to an architecture denominated ”Booster”, that can provide Medium and Low temperature cooling (MT and LT). Today, recent and common adopted innovative technology has come in the form of including Parallel Compression (PC), Multi-Ejectors (ME) and different Sub-cooling Methods in the system architecture. Some authors have classified these in three development generations: 1^{st} generation, Booster Layout; 2^{nd} generation, PC; and 3^{rd} generation, ME (Gullo et al., 2018).

Mainstream attention is leaning primarily towards ejector solutions, such as shown by Gullo et al. (2018). However, in this context, the authors of the present paper have noticed that in recent open literature there has been a relative disregard towards possible Vapour Injection (VI) solutions for supermarket refrigeration. Two-Stage compression systems using rolling-piston compressors, which this paper focuses on, and the more recently developed transcritical

VI scroll compressor technology can allow for such a system architecture (Dickes et al., 2022). Two-Stage compression with VI has already been studied in open literature to a certain extent. On one hand, some CO_2 VI Heat-Pump (HP) applications have been studied (Baek et al., 2014a) (Baek et al., 2014b) (Pitarch et al., 2016). On the other hand, studies covering the food-retail cooling-demand temperature range have also been developped (Hwang et al., 2004) (Cavallini et al., 2005) (Cecchinato et al., 2009). Within these research work, some interesting coupling of this architecture has been done with mechanical sub-cooling, such as Liu et al. (2019), expanders, such as Liu et al. (2017), and ejectors, such as Xing et al. (2014). On the other side, CO_2 Two-Stage Compressors for adapted for VI have already been developed and commercialized by industrial manufacturers (Mizuno et al., 2017) (Tashibana, 2015).

This work presents an experimental study on a condensing unit for supermarket refrigeration using a rolling piston two-stage compressor that can cover MT or LT demand. On one hand, one objective of the experimental campaign is to assess the system performance in various operating conditions. On the other hand, the system has been instrumented in order to characterize the compressor performance and calibrate and fully validate a semi-empirical model that has been described in a recently published paper.

2. CASE STUDY AND TEST RIG

2.1 General scope

The studied system is a commercial Condensing Unit for supermarket refrigeration. The system architecture includes a two-stage rolling piston compressor, inter-cooling and flash tank Vapour Injection (FTVI), as shown in Figure 1. The architecture follows the logic of a decentralized supermarket refrigeration system, and thus, can cover just one single cooling demand at a given temperature. The system has been instrumented to measure two out of the three mass flow rates of the compressor, the third one being deducible from the collected data. Pressure sensors are installed to measure

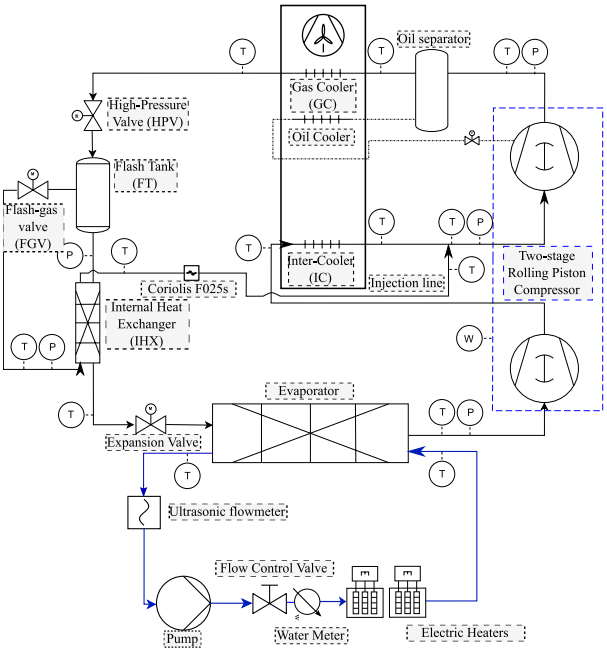

Figure 1: System Architecture

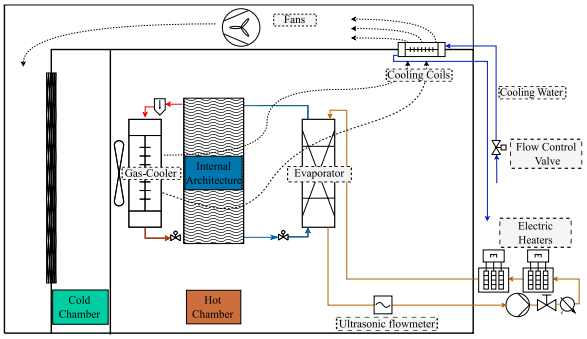

Figure 2: Climatic Chamber used to control the system boundary conditions

the flash tank, gas-cooler, intermediate compressor and evaporating pressures. Only the intermediate pressure level has two measuring points: one at the first stage compressor discharge and the other at the second stage suction. Contact thermocouples are installed on the piping of the system, with due thermal insulation from the ambient temperature. Electric power supplied to the compressor has been measured directly using a power analyzer. A coriolis mass flow meter measures the injection mass flow rate coming from the internal heat exchanger (IHX). Operating conditions in the water-glycol loop that simulates the cooling demand are controlled by varying the water-glycol mass flow rate and the power supplied by the electric heaters of up to 18 kW of nominal capacity. The ethylene glycol-water solution is a 60% volume based mixture whose flow rate is measured by means of a water meter and an ultrasonic flow meter. The

supply air temperature to the condensing unit flows in a closed loop where it heats in the gas-cooler and inter-cooler and then is cooled by a air-water fins and coil heat exchanger, as shown in Figure 2. The supply air temperature is then controlled by changing the cooling water mass flow rate. Steady state points were recorded during 15 minutes each. Table 1 shows a summary of different sensors of interest and their respective nominal accuracy. The uncertainty propagation is computed through the Python package *uncertainties* for the physical quantities of interest (Lebigot, 2016).

Table 1: Sensors especifications in the test rig

Variable	Transducer	Accuracy	Range
Temperature	T type thermocouple	±1.0 [°C]	-185...+300 °C
Pressure	PT5-50M pressure transmitter	±0.5 [bar]	0...50 [bar(g)]
	PT5-150D pressure transmitter	±1.5 [bar]	0...150 [bar(g)]
Mass Flow Rate	Coriolis F025s	±(0.5%) of reading	0...2720 [kg/h]
Water Volumetric Flow Rate	Optisonic 6300P	±(3.0%) of reading	0...20 [m/s]
	Water meter	±(2.0%) of reading	0...3[m^3/h]
Electric Power	EXTECH 1200A	±(2.0% +0.008 kW) of reading	0...10 [MW]
Compressor rotating speed	Inverter	±(0.1) [Hz]	30...60 [Hz]

2.2 Test Results.

The test plan has been executed mostly aiming at obtaining different sets of $T_{gc,out}$ temperatures rather than setting T_{amb}. This would comparing the thermodynamic cycle at different operating points more independently of the heat exchange efficiency at the gas-cooler. The tested range of $T_{gc,out}$ goes from 24 to 40 [°C]. The second system boundary condition is the cooling capacity, which is varied between 6.9 to 17.4 [kW]. The aim is mainly to assess the performance of the system at partial load and characterize de compressor performance at various rotational speeds. However, since the operator did not have a direct control on the compressor speed and the only controllable actuator on the refrigerant side is the expansion valve, to maintain a constant evaporating temperature proved difficult. 40 steady-state points have been performed. A p-h diagram of one subcritical steady-state is presented in Figure 3 to illustrate the thermodynamic cycle. The condensing unit control has been set to maintain what is commonly defined as medium temperature evaporating conditions, of about -8 to -10 [°C]. This corresponds roughly to the operating conditions to preserve from vegetables and fruits up to meat and fish. An overview of the test results is presented in Figure 4. In this work, the interest is mostly focused on the thermodynamic cycle performance. Hence, COP is defined as only considering the compressor electric power input, as in Equation 1. It is considered that the highest cooling capacity measuring accuracy comes from the electric power input of the electric heaters of the closed water-glycol loop showed in Figures 1 and 2. The whole circuit is thermally insulated, in consequence, ambient heat gains are neglected. A cross-check of the measured cooling capacity $\dot{Q}_{ev,w}$ using the mass flow, specific heat and temperature difference across the evaporator, versus the electric power input of the heaters $\dot{Q}_{ev_w,el}$ has been performed, showing good match. COP measured results show a variation from 3.6 at $T_{gc,out} = 24[°C]$ to 1.3 at $T_{gc,out} = 40[°C]$, following an almost linear decrease for the tested operating conditions.

$$COP = \frac{\dot{Q}_{ev,w,el}}{\dot{W}_{cp,el}} \tag{1}$$

When in subcritical operation, $\Delta T_{appr,gc}$, defined in Equation 2, is of around 6-8 [K]. For these conditions, most of the operating points present a gas-cooler exhaust sub-cooling of less than 1.6 [K]. When the system operates transcritical gas cooler pressures, $\Delta T_{appr,gc}$ decreases to 2-4 [K]. Regarding P_{gc} control, in the subcritical region, the pressure rises linearly with $T_{gc,out}$ increase up to the critical pressure. From there, there is a clear boundary in the control and behaviour of the condensing unit. Since $\Delta T_{appr,gc}$ drops so rapidly, it has proven difficult to perform steady state tests in between $T_{gc,out} = 29[°C]$ and $T_{gc,out} = 35[°C]$. From that point, pressure control seems to have a linear relation to $T_{gc,out}$, as it is the common practice in other CO_2 system architectures control.

Resulting pressure ratios across the two-stage compressor range from 2.35 to 4.08. Pressure ratios are higher for the first stage of compression than for the second one, ranging from 1.83 to 2.71, in contrast to 1.17 to 1.62. The intermediate pressure $P_{ex,cp,1}$ should be heavily influenced by the displacement volumes ratio between the first and second stage of compression, as shown by Vega et al. (2021b). High intermediate and injection pressure should imply a smaller second

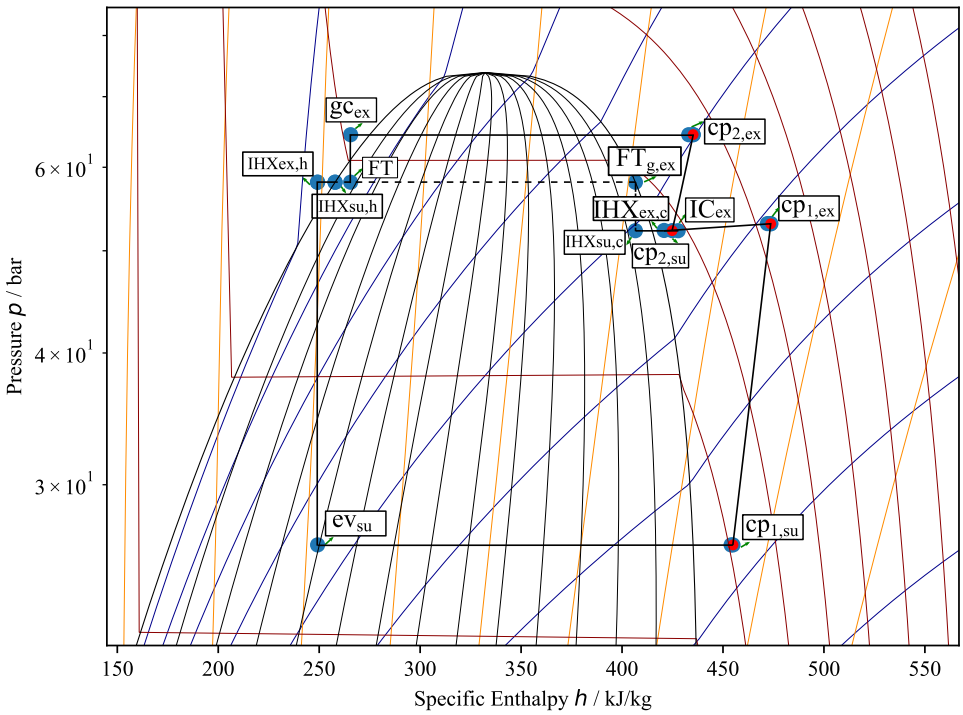

Figure 3: P-h diagram of the thermodynamic cycle in a subcritical operating point.

stage displacement volume, as a agreement between density and swept volume occurs when trapping the refrigerant. On the otherside, to allow for VI, the control of the flash-gas valve (FGV) must be done in order to maintain a higher P_{FT} pressure than $P_{su,cp,2}$. For this reason, P_{FT} is rather high across all operating points, ranging from 58-60 [bar(a)] in subcritical operation, up to 72.6-74.6 [bar(a)] for high $T_{gc,out}$ conditions, surpassing the critical point.

$$\Delta T_{appr,gc} = T_{gc,out} - T_{amb} \tag{2}$$

The internal heat exchanger function has a triple function of increasing cooling capacity, providing sub-cooling at the evaporating valve inlet, and superheat at the injection point. For most of the operating points, a sub-cooling higher than 1 [K] results from the IHX, with a median of 1.76 [K]. However, regarding the superheat at the outlet of the cold side of the IHX, there are 20 operating points where the nominal value of superheat at the injection point is lower than the calculated uncertainty. In this scenario, it is then considered that two-phase flow may be present in these cases. The determination of the thermodynamic state is then calculated as described in the following sections.

3. SEMI-EMPIRICAL TWO-STAGE ROLLING PISTON COMPRESSOR MODEL

A semi-empirical modelling approach has recently been applied to a Two-Stage Rolling Pistons Compressor using CO_2 (Vega et al., 2021a). However, at the time, the authors had neither have vapour injection data nor discharge temperature data to validate the model fully. Also, the previous case-study used to partially validate the model was a compressor with high-pressure shell, whereas in the present study the compressor is designed with a intermediate-pressure shell. Thus, the present study serves to further validate the proposed model, described in Figure 5. A detailed description of the model equations can be found at the related work of Vega et al. (2021a). In this study, the effect of the inter-cooler into the compressor is taken into account by introducing a new thermodynamic state at Point 6b in Figure 5. Thus, the heat exchange (inter-cooling) between Point 6 and 6b does not interact with the isothermal wall or any of the compression processes directly. Since in the present study the vapour-injection occurs at the exterior of the compressor and no injection port is present, the modelling element characterized by A_{inj} is not considered. Thus, the injection thermodynamic state is an input of the model and the resulting injection mass flow is determined by the mixing state at Point 7 and the subsequent density after the heat exchange and leakage/re-expansion mixing involving

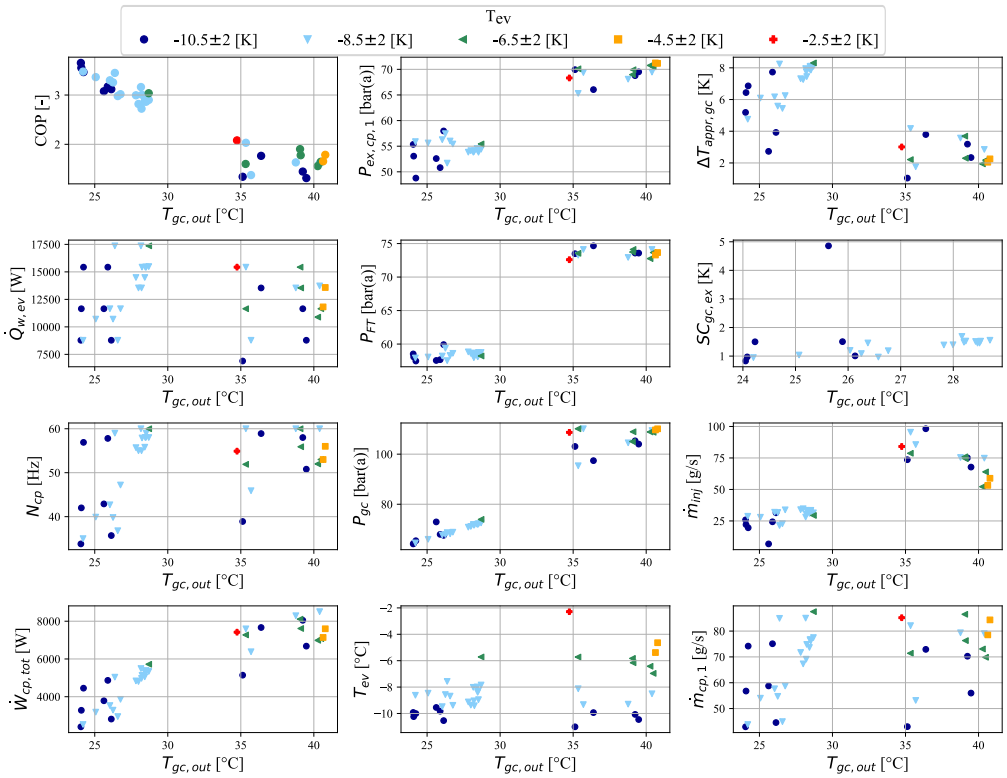

Figure 4: Condensing unit tests overview. Data is grouped according to evaporating temperature bins.

Points 8 and 9.

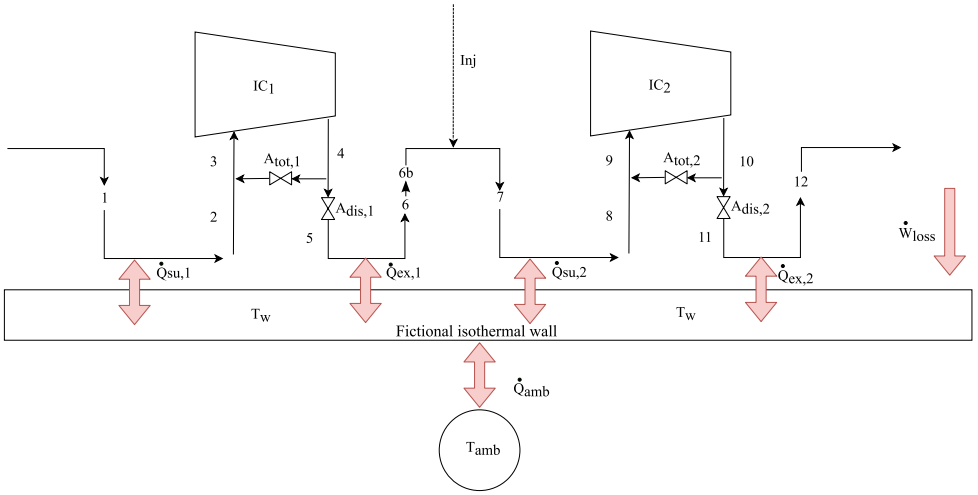

Figure 5: Semi-Empirical Two-Stage Rolling Pistons Compressor Model

3.1 Model calibration procedure and parameter results.

The model has 13 parameters that have to be identified by means of an error objective function to minimize, described in Equation 3. Notably, the displacement volume of the 2^{nd} stage of compression is not indicated by the compressor manufacturer, and thus, will be identified as a model parameter by means of the before-mentioned objective function. The 1^{st} stage displacement volume is known from manufacturer data and corresponds to 20.8 cm^3. 40 steady-state

points have been performed, from which a sub-group of 13 have been chosen for model calibration. Thus, the 27 remaining points are used to verify the accuracy of the model. The points selection for model calibration has been done taking care of covering a wide range of R_p, compressor speed, mass flows and compressor electric power input. The model has been implemented Python, using *CoolProp* 6.3.0 bi-cubic interpolation to calculate the R744 thermophysical properties Bell et al. (2014). The reference mass flow rate, $\dot{m}_{ref}$, is set too be $V_{IC,1} \cdot N_{ref} \cdot \rho(T = 273.15[K], P = P_1)$. The resulting parameters from the error minimization procedure are detailed in Table 2.

$$g = \sqrt{\frac{1}{n}\sum_{i=1}^{n}\left[\left(1-\frac{\dot{m}_{su,cp,calc,i}}{\dot{m}_{su,cp,mes,i}}\right)^2+\left(1-\frac{\dot{m}_{inj,cp,calc,i}}{\dot{m}_{inj,cp,mes,i}}\right)^2+\left(1-\frac{\dot{W}_{cp,calc,i}}{\dot{W}_{cp,mes,i}}\right)^2+\left(1-\frac{T_{dis,calc,i}}{T_{dis,mes,i}}\right)^2\right]} \tag{3}$$

Table 2: Identified Parameters of the compressor model resulting from the error minimization procedure.

Parameter	Bounds	Result	Units
UA_{amb}	0.1-3.4	0.760	[W·K^{-1}]
$UA_{su,ref,1}$	3-25.5	4.23	[W·K^{-1}]
$UA_{ex,ref,1}$	1- 25.5	21.3	[W·K^{-1}]
α_1	0.06-0.35	0.33	[-]
$A_{leak,1}$	0.030-0.170	0.14	[mm^2]
$A_{dis,1}$	0.050-37.4	13.18	[mm^2]
$UA_{su,ref,2}$	1-25.5	13.4	[W·K^{-1}]
$UA_{ex,ref,2}$	3-25.5	8.39	[W·K^{-1}]
α_2	0.06-0.35	0.28	[-]
$A_{leak,2}$	0.030-0.170	0.061	[mm^2]
$A_{dis,2}$	0.050-37.4	16.1	[mm^2]
$V_{IC,2}$	4.00-14.0	12.0	[cm^3]
$\dot{W}_{loss,SBY,ref}$	40-240	213.1	[W]

3.2 Results and model validity testing.

Figure 6 compares the predicted and the measured values of the suction mass flow rate at the 1st compression stage. Half of the points present a maximum deviation of 4.8% with respect to experimental values, whilst only 2 points have a deviation higher than 10%. However, the VI mass flow rate prediction present considerably higher error with the current set of model parameters, as shown in Figure 7. The median of the absolute error is of 28.7 %, only 4 points within an absolute error below of 10% and a maximum absolute error of 88%. One of the possible explanations for this is that the 2nd stage displacement volume, $V_{IC,2}$, the most important parameter to predict the injection mass flow, is not known and it is one of the parameters determined by error minimization. On the other hand, several operating points present little or no superheat at the injection point. In this cases, the determination of the thermodynamic state is not done as a function of pressure and temperature, but it is calculated as a function of pressure and enthalpy. For these cases, the enthalpy of the injection point is calculated by doing an energy balance around the IHX as described by Equation 4, by assuming that the inlet enthalpy of the cold side in the IHX is the enthalpy of the saturated gas coming out of the Flash Tank if this is in subcritical conditions, or a function of pressure and temperature if otherwise. Despite this is theoretically possible, the temperature drop in the hot side of the IHX, with a median of 1.8 [K], is too low to perform anaccurate energy balance, considering the uncertainties involved when using T thermocouples, as described in Table 1. This would introduce further errors to the prediction of the injection mass flow rate, as the thermodynamic states that serve as some inputs of the model may be ill-determined for the model calibration procedure and validation calculations, specially in a zone where the density gradients are high.

$$h_{inj} = \begin{cases} h_g(P_{FT}) + \frac{\dot{m}_{su,cp,1,mes}}{\dot{m}_{inj,cp,mes}} \cdot \left[h(P_{FT}, T_{h,su,IHX}) - h(P_{FT}, T_{h,ex,IHX})\right], & \text{if } P_{FT} < P_{crit} \\ h(P_{FT}, T_{c,su,IHX}) + \frac{\dot{m}_{su,cp,1,mes}}{\dot{m}_{inj,cp,mes}} \cdot \left[h(P_{FT}, T_{h,su,IHX}) - h(P_{FT}, T_{h,ex,IHX})\right], & \text{if } P_{FT} \geq P_{crit} \end{cases} \tag{4}$$

In spite of this, error on the prediction of the total discharge mass flow rate of the compressor are still limited, as shown in Figure 8. The 25th, 50th and 75th percentiles of the points have an absolute error of the discharge mass

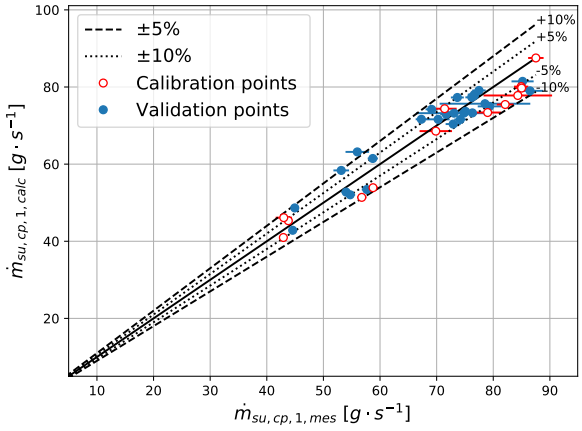

Figure 6: Parity plot of first stage compression suction mass flow rate.

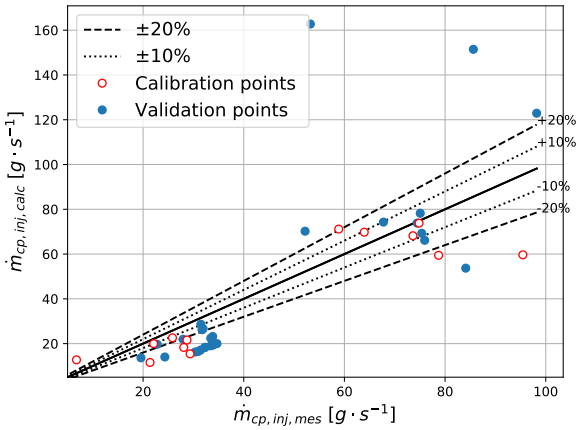

Figure 7: Parity plot of the injection mass flow rate.

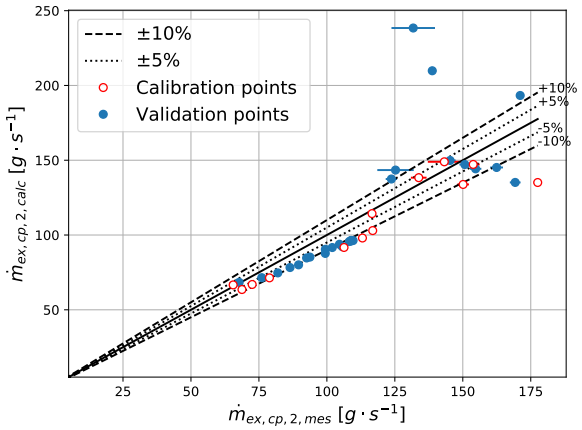

Figure 8: Parity plot of the total discharge mass flow at second stage compression.

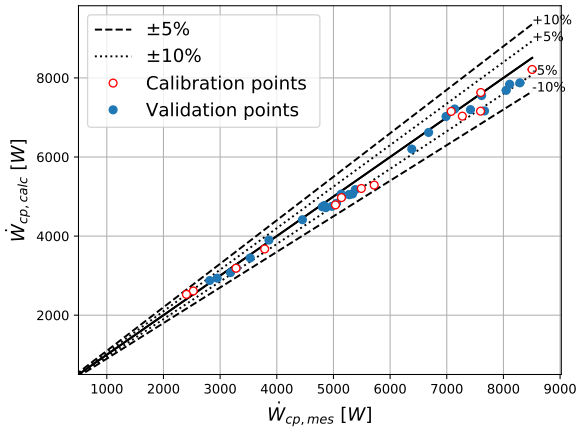

Figure 9: Parity plot of the total electric power input to the compressor.

flow rate prediction lower than 7.38%, 10.35% and 12.0%. The compressor electric power input prediction present very good results as 75% of the points present an absolute error below 4.41%. Lastly, regarding the compressor 2_{nd} stage discharge temperature model prediction, the 25th, 50th and 75th percentile errors are respectively 5.0, 8.46 and 9.5 [K]. This temperature prediction results are higher than the ones from Dardenne et al. (2015), which were limited mostly at ±5 [K] for a VI scroll semi-empirical compressor model. However, differences may once again be explained by the VI thermodynamic state points definition as previously explained. In summary, first stage suction mass flow rate, second stage total discharge mass flow rate and electric power consumption of the compressor are variables that are satisfactorily predicted by this semi-empirical model. Regarding injection mass flow rate prediction, results show high error percentages. However, the combined effect of not having the second stage displacement volume information as a model parameter, plus many possible ill-defined injection thermodynamic states as model input, suggest that the available data is not well adapted to perform a rigorous model validation.

4. WORK PERSPECTIVES

Regarding the semi-empirical two-stage compressor model validation, one of the main work perspectives is to obtain more reliable data regarding the injection point thermodynamic state. This would most likely allow for better results in the injection mass flow rate and second stage discharge temperature prediction. Also, this would most likely lead to a more accurate second stage displacement volume determination by the error minimization procedure. Regarding

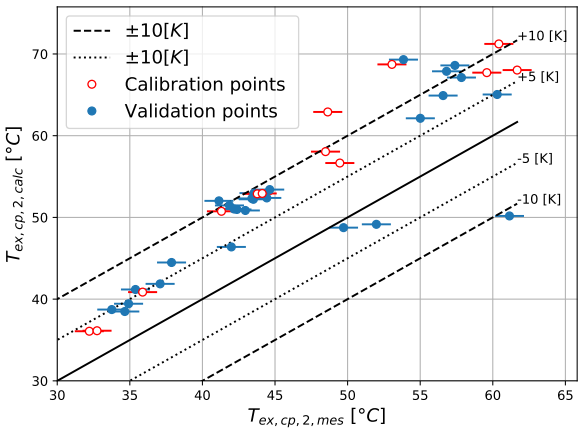

Figure 10: Parity plot of the second stage discharge temperature.

this, a sensitivity analysis must be performed to assess the impact of this unknown important parameter on the overall model results.

With respect to the analysis of the condensing unit from a system point of view, a second test campaign must be performed to obtain data at lower evaporating temperatures, ideally at -35 to -30 [°C]. Then, an analysis on the optimal control of the system variables must be performed, specially gas cooler and flash tank pressure control. It would also be interesting to compute the theoretically optimum displacement volumes ratio between the second an first stage of compression for different operating points and compare it to the results of the system cycle studied by Vega et al. (2021b). A quasi-optimum design could be then proposed for different different evaporating temperatures and climate conditions.

5. CONCLUSIONS

- A commercial CO_2 condensing unit for supermarket has been tested in a climatic chamber. The test rig has been instrumented with the priority of assessing the compressor performance, as well as the cycle performance. 40 experimental points have been performed where the main boundary conditions varied are outlet gas cooler temperature and cooling capacity. Thus, experimental points with $T_{gc,out}$ ranging from 24 to 40 [°C], and with $\dot{Q}_{ev}$ ranging from 6.9 to 17.4 [kW] have been performed. Tests have been performed at medium evaporating temperatures, with most of the points at -8 to -10 [°C].
- Measured COP ranges from 3.6 at $T_{gc,out}$ = 24 [°C] to 1.3 at $T_{gc,out}$ = 40 [°C] at T_{ev} = - 10 [°C].
- A rapid decrease of the outlet gas cooler approach temperature to the ambient temperature when passing to transcritical operation has introduced difficulties to obtain steady-state points at $T_{gc,out}$ between 29 and 35 [°C].
- The high pressure control valve, regulates as to obtain low subcooling, of about 1-2 [K] in subcritical conditions. In transcritical operation, gas-cooler pressure control follows a linear relationship with respect to $T_{gc,out}$.
- The second stage compression displacement volume is unknown. Intermediate compressor pressure $P_{su,cp,2}$ and flash tank pressure P_{FT} are rather high, specially at high $T_{gc,out}$. This suggests the ratio of the second to the first compression displacement volumes is rather small. This is also what the semi-empirical compressor model identified parameters indicate.
- A semi-empirical two-stage compressor model has been calibrated with the experimental data to characterize the compressor performance and being able to extrapolate it. An objective function is established to identify the 13 model parameters by error minimization on the prediction of first stage suction mass flow rate, injection mass flow rate, total electric power input and second stage discharge temperature. Notably, an effort to identify the unknown second stage displacement volume is done, as it is one of the main design parameters of the system as a whole. A sub-group of 13 experimental points has been selected for model calibration, leaving the rest for testing the model validity. Results show an acceptable prediction of the the first stage suction mass flow rate, total discharge mass flow rate and the electric power consumption, with average absolute relative errors of 6.2 %, 10.2 % and 4.4 %. However, in the case of injection mass flow rate prediction and second stage discharge temperature,

this figures are as high of 28.5% (mean absolute relative error) and 8.0 [K] (mean absolute error) respectively. This deviations may be explained by many possibly ill-defined thermodynamic states at the injection point that serve as input for the model.

- Work perspectives that arise are to find operating regions with enough superheat in the injection point, so a more rigorous test of the validity of the semi-empirical compressor model is possible. Secondly, a test campaign with lower temperature evaporating conditions should be performed. Lastly, it is of interest to perform an optimization of the thermodynamic cycle at various operating boundary conditions and compare with the actual control and design of the system.

6. NOMENCLATURE

A	Area	calc	calculated
COP	Coefficient of Performance	cp	compressor
cp	Compressor	crit	critical
ev	Evaporator	dis	discharge
IC	Inter-cooler	ev	evaporator
IHX	Internal Heat Exchanger	evValve	expansion valve
$\dot{m}$	Mass flow rate	el	electric
MT	Medium Temperature	ex	exhaust
FT	Flash Tank	FT	flash tank
P	Pressure	gc	gas cooler
g	Objective function	inj	injection
gc	Gas Cooler	IHX	internal heat exchanger
h	Specific enthalpy	liq	liquid
LT	Low Temperature	loss	electro-mechanical power loss
ME	Multi-Ejector	mes	measured
FTVI	Flash Tank Vapour Injection	out	outlet/exhaust
SCOP	Seasonal Coefficient of Performance	p	pressure
$\dot{Q}$	Heat flow	r	ratio
R	Ratio	rec	recovered
SC	Sub-cooling	s	isentropic
T	Temperature	su	supply
UA	Overall heat transfer coefficient	SBY	stand-by electromechanical loss
V	Displacement Volume	tot	total
$\dot{W}$	Power	w	water-glycol or fictious isothermal wall
α	Power loss proportionality coeff.	1	1^{st} stage of compression or 1^{st} thermo-
Subscript		dynamic state point	
amb	ambient	2	2^{nd} stage of compression or 2^{nd} thermo-
appr	temperature approach	dynamic state point	

REFERENCES

Baek, C., Heo, J., Jung, J., Cho, H., and Kim, Y. (2014a). Effects of the cylinder volume ratio of a twin rotary compressor on the heating performance of a vapor injection CO2 cycle. *Applied Thermal Engineering*, 67(1):89 – 96.

Baek, C., Heo, J., Jung, J., Lee, E., and Kim, Y. (2014b). Effects of vapor injection techniques on the heating performance of a CO2 heat pump at low ambient temperatures. *International Journal of Refrigeration*, 43:26 – 35.

Bell, I. H., Wronski, J., Quoilin, S., and Lemort, V. (2014). Pure and pseudo-pure fluid thermophysical property evaluation and the open-source thermophysical property library coolprop. *Industrial & Engineering Chemistry Research*, 53(6):2498–2508. PMID: 24623957.

Cavallini, A., Cecchinato, L., Corradi, M., Fornasieri, E., and Zilio, C. (2005). Two-stage transcritical carbon dioxide cycle optimisation: A theoretical and experimental analysis. *International Journal of Refrigeration*, 28(8):1274 – 1283.

Cecchinato, L., Chiarello, M., Corradi, M., Fornasieri, E., Minetto, S., Stringari, P., and Zilio, C. (2009). Thermodynamic analysis of different two-stage transcritical carbon dioxide cycles. *International Journal of Refrigeration*, 32(5):1058 – 1067.

Dardenne, L., Fraccari, E., Maggioni, A., Molinaroli, L., Proserpio, L., and Winandy, E. (2015). Semi-empirical modelling of a variable speed scroll compressor with vapour injection. *International Journal of Refrigeration*, 54:76 – 87.

Dickes, R., José, C. D., Vega, J., and Winandy, E. (2022). Lab Testing of a Retroffited CO2 Booster Rack with Transcritical Scroll Compressors featuring Dynamic Vapour Injection. Purdue University, The United States of America. Purdue e-Pubs.

Gullo, P., Hafner, A., and Banasiak, K. (2018). Transcritical R744 refrigeration systems for supermarket applications: Current status and future perspectives. *International Journal of Refrigeration*, 93:269 – 310.

Hwang, Y. H., Celik, A., and Radermacher, R. (2004). Performance of CO2 Cycles with a Two-Stage Compressor. In *International Refrigeration and Air Conditioning Conference*. Purdue e-Pubs.

Lebigot, E. (2016). Uncertainties: a Python package for calculations with uncertainties. `http://pythonhosted.org/uncertainties/`.

Liu, S., Lu, F., Dai, B., Nian, V., Li, H., Qi, H., and Li, J. (2019). Performance analysis of two-stage compression transcritical CO2 refrigeration system with R290 mechanical subcooling unit. *Energy*, 189:116143.

Liu, S., Sun, Z., Li, H., Dai, B., and Chen, Y. (2017). Thermodynamic analysis of co2 transcritical two-stage compression refrigeration cycle systems with expanders. *HKIE Transactions*, 24(2):70–77.

Mizuno, H., Murakami, K., Kawanishi, A., Ichigaya, K., Ikeda, M., and Enya, A. (2017). Development of HCCV1001 Commercial Condensing Unit Employing CO2 as Natural Refrigerant. Technical review, Mitsubishi Heavy Industries.

Pitarch, M., Navarro-Peris, E., Gonzalvez, J., and Corberan, J. (2016). Analysis and optimisation of different two-stage transcritical carbon dioxide cycles for heating applications. *International Journal of Refrigeration*, 70:235 – 242.

Skačanová, K. Z. and Battesti, M. (2019). Global market and policy trends for CO2 in refrigeration. *International Journal of Refrigeration*, 107:98 – 104.

Tashibana, H. (2015). Introduction of Panasonic New CO2 refrigeration system (Technical Part). Atmosphere asia 2015 report, Panasonic Corporation - Refrigeration and Air-Conditioning Devices Business Division.

Vega, J., Cuevas, C., Dickes, R., and Lemort, V. (2021a). Application of a semi-empirical modelling approach to a two-stage rotary CO2 compressor. In *9th IIR Conference on Ammonia and CO2 Refrigeration Technologies*. International Institute of Refrigeration IIR.

Vega, J., Davila, C., and Lemort, V. (2021b). Two-stage Compression With Vapor Injection: A Study On A Disregarded Solution In CO2 Booster Applications For Supermarket Refrigeration. In *International Refrigeration and Air Conditioning Conference*. Purdue e-Pubs.

Xing, M., Yu, J., and Liu, X. (2014). Thermodynamic analysis on a two-stage transcritical co2 heat pump cycle with double ejectors. *Energy Conversion and Management*, 88:677 – 683.

ACKNOWLEDGMENT

This work was funded by the National Agency for Research and Development (ANID) / Scholarship Program / DOCTORADO BECAS CHILE/2017 - 72180512.